Estimating PAH Dry Deposition by Measuring Gas and Particle Phase Concentrations in Ambient Air

Kuan-Foo Chang[1], Guor-Cheng Fang[2]*, Chungsying Lu[1] and Hsunling Bai[3]

[1]*Department of Environmental Engineering, National Chung-Hsing University, Taichung 402, Taiwan*

[2] *Air Toxic and Environmental Analysis Laboratory, Hungkuang University, Sha-Lu, Taichung 433, Taiwan*

[3] *Institute of Environmental Engineering, National Chiao-Tung University, Hsinchu 300, Taiwan*

Concentrations of the total polycyclic aromatic hydrocarbons (PAHs) in both the gas-phase and particle-phase were measured simultaneously in industrial, urban and suburban areas, and were 1652, 1185, and 834 ng/m^3, respectively. PAHs with two to four-ring were distributed more than 94% in the gas-phase of all sampling sites. Meanwhile, for PAHs with five to seven-ring, less than 70% were distributed in the gas-phase of the three sites. Approximately two-thirds of the three most hazardous PAHs (BbF + BaP + DBA) were distributed in the gas-phase at the TIP and NCHU, and only one-third of BbF + BaP + DBA were distributed in the gas-phase at the THU. Total dry deposition flux was mainly contributed, with a proportion of between 53.3% and 63.4%, by PAHs with three to four-ring at the three sites. For LMW PAHs, the gas-phase PAHs contribute over 87% to the dry deposition flux at the three sites. Meanwhile, the particle-phase PAHs contribute more than 86% and 99% to the dry deposition flux of the MMW and HMW PAHs, respectively. The mean dry deposition velocities were 0.01, 0.24, 0.47, 0.76, 0.84 and 0.88 cm/s for two to seven-ring PAH homologue. Notably, the dry deposition velocity of the HMW PAHs was significantly higher than that of the LMW PAHs at the three sampling sites. The dry deposition velocities of BbF + BaP + DBA PAHs were 0.8, 0.64 and 1.02 cm/s at the TIP, NCHU and THU, respectively. Accordingly, hazardous PAHs with high dry deposition velocities are threatening to human health by dry deposition.

Keywords: PAHs, dry deposition flux, dry deposition velocity

1. Introduction

PAHs are formed during incomplete combustion or pyrolysis of organic material and are related to the use of oil, gas, coal and wood in energy

production. Other contributors to ambient air levels include indoor smoking and heating (WHO, 1987). PAHs recently have received attention in air pollution studies because some of these compounds are highly carcinogenic or mutagenic. Particularly, benzo[a]pyrene (BaP) has been identified as a carcinogen. Reliable sampling and analytical methods are required to understand the extent of human exposure to BaP and other PAHs (USEPA, 1999). Generally, atmospheric PAHs are partitioned

---

between gas and particulate matter and associated as aerosol. Accordingly, breathing PAHs can represent a health hazard for humans. Given this health concern, monitoring PAHs levels in urban areas is increasingly important (Chetwittayachan *et al.* 2002). High concentrations of atmospheric PAH exist in the urban environment, because of high vehicle density and dispersion of atmospheric pollutants. Consequently, the risk associated with human exposure to atmospheric PAH is high in cities (Caricchia *et al.* 1999). Despite the significant reduction of urban pollution owing to reduce coal usage and a shift toward other fossil fuels (oil or natural gas) for domestic heating, the urban development and traffic density, has increased urban pollution. Furthermore, particulates produced by automobiles are significantly smaller than coal particulates and have a higher fraction breathable size (Manoli *et al.* 2002). This information forces a new emphasis on multi-ring heavier PAHs, which usually adsorbed on the small particulates. However, the lighter PAHs are abundant in the urban atmosphere and can react with other pollutants to form more toxic derivatives (Park *et al.* 2002).

Dry deposition is a major pathway for PAH transfers from air to land and water. Interest in atmospheric deposition has grown over the past decade because of concerns regarding the health effects resulting from the deposited material entering the environment. Dry deposition can be measured using a smooth plate with a sharp leading edge mounted on a wind vane pointing into the wind. Because the smooth plate provided a minimum air flow disruption and a good estimation of low for dry deposition flux, its collection surface was modeled after those used in wind tunnel studies (Holsen *et al.* 1991). However, Noll (1989) and Sehmel (1980) have designed mathematical models of deposition velocity for atmospheric particles. These models have been applied successfully in several investigations (Fang *et al.* 1999; Sheu *et al.* 1997) on forecasting dry deposition flux.

Ambient air PAHs in the gas-phase and particle-phase was measured in Taichung Industrial Park (TIP), in downtown Taichung (National Chung-Hsing University, NCHU) and in suburban Taichung (Tunghai University, THU). The dry deposition velocities of PAHs, which were measured by Sheu *et al.* (1997), also were applied to estimate the dry deposition flux of PAHs in these three sampling sites in central Taiwan.

2. Experimental Method

2.1 Sampling Program

Three sampling sites, Taichung Industrial Park (TIP), urban site (NCHU) and suburban site (THU) were selected to characterize ambient air PAH concentrations. TIP is a typical large-scale industrial park in Taiwan. TIP occupies 580 hectares and contains over eight hundred factories, including factories in the chemical, petroleum, plastic, and electronics industries. The sampling site selected was the roof of a pharmaceutical factory (15 m in height), located at the center of the TIP. The THU sampling site, located on top of a hill near the TIP, was surrounded by vegetation and the immediate area contained roughly 15,000 students and faculty. However, the vicinity also contained the incinerator of Taichung Veterans General Hospital (a significant combustion source) and a major local highway located west of Tunghai University. The sampling height was in the range 1-1.5 m above ground level to simulate the human breathing zone. Finally, the NCHU sampling area, located in downtown Taichung, had two heavy-traffic local highways pass through it. The sampling height was around 10 m, with the samples being taken on the roof of the Environmental Engineering building of NCHU, located close to a major highway. Table 1 illustrated the detailed sampling conditions.

Table 1. Sampling information

Sampling date	Temperature (℃)	Relative humidity (%)	Wind speed (m/s)	Wind direction	Atmospheric pressure (Pa)
1-3 August 2002	33	65	1.6	NW	1003.5
13-15 August 2002	39	63	1.3	N	1004.6
19-21 August 2002	38	63	0.9	N	1007.9
25-27 September 2002	28	65	1.8	NE	1012.1
7-9 October 2002	25	54	5.2	NW	1012.3
9-11 October 2002	31	57	2.0	NNE	1014.2
28-30 Octerber 2002	28	58	1.7	N	1013.5
1-3 November 2002	27	71	2.3	N	1013.8
4-6 November 2002	24	44	1.3	N	1020.4
4-6 December 2002	25	64	0.7	NNW	1018.1
9-11 December 2002	16	59	3.5	N	1023.8
11-13 December 2002	20	68	3.5	N	1024.3
Mean	27.8	60.9	2.2	-	1014.0
Standard deviation	6.7	7.2	1.3	-	6.8

Samples were gathered using three PS-1 samplers (GPS1 PUF Sampler, General Metal Work) with a pump drawing air through a tissue quartz filter (2500 QAT-UP, Dimension 102 mm). Before sampling, filters were oven baked at 450 ℃ for 8 h to remove organic impurities. Glass cartridges were cleaned by sequential Soxhlet extractions with distilled-deionized water, methanol, dichloromethane (DCM) and a mixture of DCM/n-hexane (50/50, v/v) for 24 h successively and finally dried in a clean oven at 45 ℃ to remove residual solvent. Particle-phase PAHs were first filtered on the tissue quartz filter. Then, Gas-phase PAHs were collected using glass cartridge, which contained a 5 cm length of polyurethane foam (PUF) plug, a 3 cm thickness of XAD-16 resin (Amberlite), and finally a 2 cm long PUF plug. During sample transportation and storage, the PUF plug and resin were stored in a clean jar wrapped with aluminum foil and the filters were placed in a sealed CD box. The filters were weighed before and after sampling to measure the particulate collected.

2.2 PAHs Analysis

Following final weighing, all filters and glass cartridges were separated in appropriate Soxhlet extractors and extracted with a DCM/n-hexane mixture (50/50, v/v) for 24 h. The extract then was concentrated under a rotary evaporator, then cleaned and re-concentrated with ultra-pure nitrogen to 1 ml as described previously by Lee *et al*. (1995). All extracts were analyzed using a gas chromatograph/mass selective detector (GC/MS, GC3800 Varian with MS2000 Saturn) with a GC capillary column (30 m × 0.25 mm × 0.25 μm, DB-5). A computer-controlled automatic sampler (Model 8200) was used together with the GC/MS system. All injections were splitless and has a volume of 1 μl. Injector and transfer line temperatures were 310 and 300 ℃, respectively. The temperature program was 35 ℃ held for 3 min, then increasing to 180 °C at 25 ℃/min and held 2 min, then increasing to 200 ℃ at 20 ℃/min and held for 2 min, and finally increasing to 300 ℃ at 2 ℃/min and being held for 6.4 min; total time was 70 min.

Twenty-one PAH compounds were quantified, with the following elution order: naphthalene (Nap), acenaphthylene (AcPy), acenaphthene (Acp), fluorene (Flu), phenanthrene (PA), anthracene (Ant), fluoranthene (FL), pyrene (Pyr), cyclopenta(c,d)pyrene (CYC), benzo(a)anthracene (BaA), chrysene (CHR), benzo(b)fluoranthene (BbF), benzo(k)fluoranthene (BkF), benzo(e)pyrene (BeP), benzo(a)pyrene (BaP), perylene (PER), indeno(1,2,3,-cd)pyrene (IND), dibenzo(a,h)anthracene (DBA), benzo(b)chrycene (BbC), benzo(ghi)perylene (BghiP) and coronene (COR).

The GC/MS was calibrated using a dilute standard solution of 16 PAH compounds (PAH Mixture-610M from Supelco) and five individual PAH compounds (from Merck Inc.) Analysis of serial dilutions of PAH standards revealed that the detection limits (DL) for individual PAH compounds were between 39 and 531 pg. The limit of quantifications (LOQ) was defined as DL divided by the sampling volume of the PS-1 sampler. Meanwhile, the LOQ of the PS-1 sampler was between 35 and 260 pg/m^3. Analysis Recovery efficiency of PAHs ranged from 77 to 98 % (average 86 %) and was analyzed using two internal standards (phenanthrene-d10 and perylene-d12).

3. Results and Discussion

3.1 PAH Concentrations in Ambient Air

Figure 1 display 21 mean concentrations of individual PAHs in both the gas-phase and particle-phase at the TIP, NCHU and THU sampling sites. The total PAHs concentrations were 1652, 1185, and 834 ng/m^3 for TIP, NCHU and THU, respectively. During the sampling period, total PAHs concentration was 4620 ng/m^3 at theTIP on December 4-6, 2002. Meanwhile, total PAHs concentrations were also high on those same
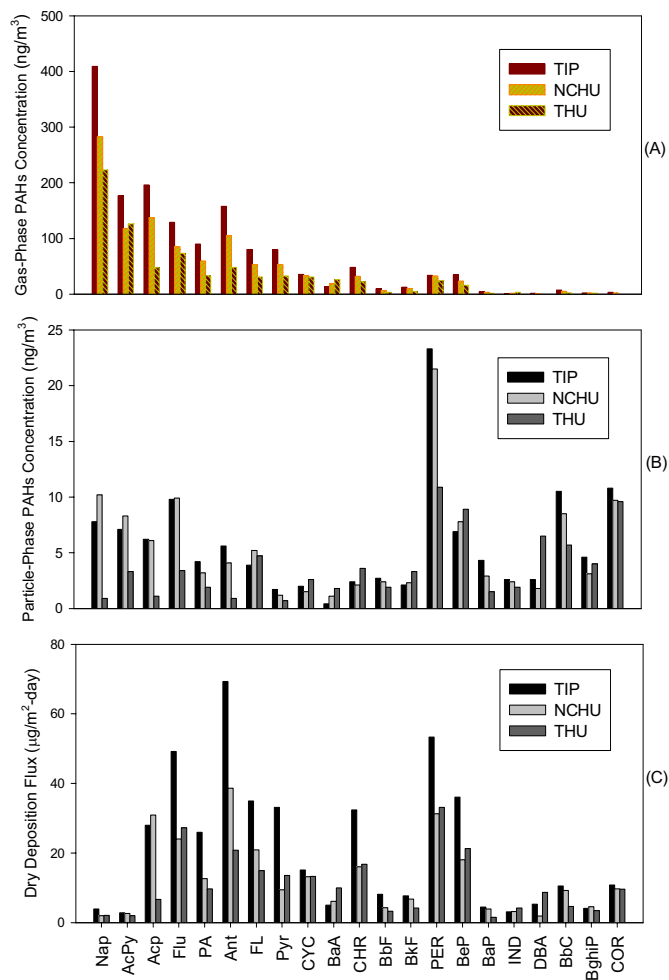
Figure 1. Values of individual PAHs at the three sampling sites, including (A) gas phase individual PAH concentration (ng/m^3); (B) particle phase individual PAH concentration (ng/m^3); (C) dry deposition flux (μg/m^2/day)

sampling days for the NCHU and THU. Owing to the burning of biomass from agricultural waste and atmospheric inversion of the city, air pollutants such as suspended particles and PAHs clearly accumulated in central Taiwan during this period. Taiwan EPA has recognized this period as the episode days.

The total PAHs gas-phase and particle-phase concentrations at the TIP were 1530 and 122 ng/m^3, respectively. These values were approximately 1.5 and 1.03 times higher than those at the NCHU and were approximately two and 1.5 times higher than at the THU. Previous studies indicated that selected PAHs (Nap, AcPy, Acp and Flu) are associated with combustion sources (Park *et al*., 2002). The sum of

Table 2. Phase distributions (%) of individual PAHs at the three sampling sites

Compound	TIP		NCHU		THU	
	Gas Phase (%)	Particle Phase (%)	Gas Phase (%)	Particle Phase (%)	Gas Phase (%)	Particle Phase (%)
Nap	98.1	1.90	96.5	3.50	99.6	0.40
AcPy	96.2	3.80	93.4	6.60	97.5	2.50
Acp	96.9	3.10	95.7	4.30	97.7	2.30
Flu	92.9	7.10	89.7	10.3	95.6	4.40
PA	95.5	4.50	94.9	5.10	94.3	5.70
Ant	96.5	3.50	96.2	3.80	98.0	2.00
FL	95.4	4.60	91.2	8.80	86.9	13.1
Pyr	97.9	2.10	97.8	2.20	97.9	2.10
CYC	94.7	5.30	95.7	4.30	92.2	7.80
BaA	97.2	2.80	94.6	5.40	93.6	6.70
CHR	95.3	4.70	93.9	6.10	86.3	13.7
BbF	78.9	21.1	73.6	26.4	63.5	36.5
BkF	85.5	14.5	81.7	18.3	58.2	41.8
PER	59.1	40.9	60.2	39.8	69.3	30.7
BeP	83.6	16.4	75.1	24.9	64.3	35.7
BaP	52.2	47.8	54.7	45.3	53.3	46.7
IND	33.3	66.7	42.9	57.1	64.2	35.8
DBA	39.5	60.5	37.9	62.1	8.5	91.5
BbC	42.0	58.0	37.5	62.5	28.8	71.2
BghiP	31.3	68.7	43.6	56.4	30.4	69.6
COR	23.8	76.2	19.2	80.8	6.8	93.2
Total-PAHs	92.6	7.40	90.3	9.70	90.5	9.50
LMW-PAHs	98.1	1.90	96.5	3.50	99.6	0.40
MMW-PAHs	95.9	4.10	94.2	5.80	95.4	4.60
HMW-PAHs	67.1	32.9	65.8	34.2	61.2	38.8
BbF + BaP + DBA	63.2	36.8	61.4	38.6	35.7	64.3

these four PAHs concentrations represented 57%, 56% and 57%, respectively, of total PAHs for each of the TIP, NCHU and THU. Consequently, combustion activities within these areas are the major contributors to PAHs concentrations in central Taiwan. However, owing to less pollutant sources at the THU, total PAHs concentrations were lower there than at the TIP and NCHU.

Total PAHs concentration highest in the gas-phase and less than 10% was distributed in the particle-phase for the three sampling sites (Table 2).

Table 2 also illustrated the phase distributions of individual PAHs at the three sampling sites. PAHs with two to four rings, such as Nap, AcPy, Acp, Flu, PA, Ant, FL, Pyr, CYC, BaA and CHR, are highest in the gas-phase of all sampling sites. However, the partition in the particle-phase increased for PAHs with high ring numbers, such as BbF, BkF, PER, BeP, BaP, IND, DBA, BbC, BghiP and COR. Because of low boiling point and high volatility, low molecular weight (LMW) PAHs (such as two-ring PAHs) and medium molecular weight

(MMW) PAHs (such as three to four-ring PAHs) are abundant in the vapor phase. Depositions of LMW and MMW PAHs on particle surfaces are relatively low compared to depositions of high molecular weight (HMW) PAHs, such as five to seven-ring PAHs (Li and Ro, 2000). Consequently, the LMW and MMW PAHs accounted for over 94% of total PAHs in the gas-phase at all sampling sites. However, the HMW PAHs accounted for less than 70 % of total PAHs in the gas-phase at all sampling sites. Table 2 also displayed the distribution of the three most hazardous PAHs (BbF + BaP + DBA) in the gas-phase and particle-phase. The partition of BbF + BaP + DBA PAHs in the gas-phase was higher at the TIP (63.2%) and NCHU (61.4%) than at the THU (35.7%). This difference occurs because of direct industrial exhaust and high levels of human activity at the TIP and NCHU sites. In comparison, approximately two-thirds of the BbF + BaP + DBA PAHs was distributed in the particle-phase at the THU. This phenomenon could occur owing to the airborne particles was transformed from distant pollution sources.

3.2 PAH Content in Ambient Particles

PAH content was determined by dividing particle-phase PAHs concentrations ($\mu g/m^3$) by the particle concentrations (g/m^3). The total-PAH content at the TIP was 2480 $\mu g/g$, higher than at the NCHU, with 2230 $\mu g/g$, or the THU, with 1240 $\mu g/g$ (Table 3). The PAH content of LMW, MMW and HMW was 6.4%, 34% and 59.6% of total particle-phase PAHs at the TIP. Notably, PAH content also increased with ring number at the other two sites. At the NCHU, the PAH content of LMW, MMW and HMW was 8.8%, 35.8% and 55.4%, resembling that at the TIP. However, the THU displayed high PAH content in the HMW with 70.3%. Owing to the photolysis reaction and higher volatility of LMW, high ring number PAHs

Table 3. Particle-phase individual PAH content in the ambient air at the three sampling sites

Compound	TIP ($\mu g/g$)	NCHU ($\mu g/g$)	THU ($\mu g/g$)
Nap	159	197	14.9
AcPy	145	161	54.5
Acp	126	118	18.2
Flu	200	192	56.2
PA	85.9	62.0	31.4
Ant	114	79.4	14.9
FL	79.7	101	77.6
Pyr	34.8	23.2	11.6
CYC	40.9	29.0	42.9
BaA	8.18	21.3	29.7
CHR	49.1	40.7	59.5
BbF	55.2	46.5	31.4
BkF	42.9	44.5	54.5
PER	476	416	180
BeP	141	151	80.9
BaP	87.9	56.1	24.7
IND	53.1	46.5	31.4
DBA	53.1	34.8	107
BbC	214	164	94.1
BghiP	94.0	60.0	66.1
COR	221	189	158
Total-PAHs	2480	2230	1240
LMW-PAHs	159	197	14.9
MMW-PAHs	843	799	354
HMW-PAHs	1480	1240	871
BbF + BaP + DBA	196	137	163

dominate in the low pollution areas following distant dispersion. This phenomenon also caused the ratio BbF + BaP + DBA PAH content to total PAH content at the THU (13%) to be approximately twice that at the TIP (7.9%) and NCHU sites (6.1%).

3.3 Calculated Dry Deposition Flux

Dry deposition flux was a combination of both gas-phase and particle-phase fluxes of PAHs, and

was calculated as follows (Lee *et al.* 1996):

$$F_T = F_g + F_p = C_g \times V_{d,g} + C_p \times V_{d,p}$$

where F_T denotes the dry deposition flux ($\mu g/m^2/day$) contributed by both the gas-phase and particle-phase, F_g represents the dry deposition flux of the gas-phase ($\mu g/m^2/day$), F_p is the dry deposition flux of the particle-phase ($\mu g/m^2/day$), C_g denotes the PAHs concentration in the gas-phase (ng/m^3), $V_{d,g}$ represents the dry deposition velocity of the gas-phase (cm/s), C_p is the PAHs concentrations in the particle-phase (ng/m^3) and $V_{d,p}$ denotes the dry deposition velocity of the particle-phase (cm/s).

Sheu *et al.* (1996) studied the dry deposition velocities of individual PAHs in both urban and petrochemical industry areas in Tainan, located in southern Taiwan. The dry deposition velocities of the industrial site in Tainan were assumed to be as that of the TIP and THU in this investigation (owing to the THU being closer to the industrial area). The dry deposition velocities of urban areas in Tainan were assumed to be as that of the NCHU. Consequently, combining with the measured atmospheric PAH concentrations, the dry deposition fluxes could be calculated, listed in Table 4. The dry deposition fluxes of individual PAHs ranged from 2.86 to 69.3, 1.90 to 38.6, and 1.55 to 33.1 $\mu g/m^2/day$ at the TIP, NCHU, and THU, respectively. The profiles of dry deposition flux of individual PAHs were very similar at the three sampling sites (Fig. 1C). This PAH pattern of dry deposition flux resembled the pattern in the particle-phase PAHs concentration (Fig. 1B) and was totally different from that in the gas-phase PAHs concentration (Fig. 1A). These results are consistent of the finding of Sheu *et al.* (1996) that the PAH dry deposition was primarily contributed by the particle-phase, even though most total PAHs existed in the gas-phase.

The dry deposition fluxes of total PAHs were

Table 4. Dry deposition flux of individual PAHs ($\mu g/m^2/day$) at the three sampling sites

Compound	TIP	NCHU	THU
Nap	3.96	2.03	2.13
AcPy	2.86	2.62	2.01
Acp	28.0	30.9	6.70
Flu	49.2	24.0	27.2
PA	26.0	12.6	9.70
Ant	69.3	38.6	20.8
FL	35.0	20.9	14.9
Pyr	33.1	9.42	13.6
CYC	15.1	13.2	13.3
BaA	5.03	6.14	10.0
CHR	32.4	16.0	16.8
BbF	8.18	4.32	3.32
BkF	7.64	6.75	4.16
PER	53.3	31.3	33.1
BeP	36.1	18.1	21.3
BaP	4.51	3.93	1.55
IND	3.07	3.23	4.17
DBA	5.28	1.90	8.71
BbC	10.5	9.28	4.63
BghiP	4.11	4.61	3.50
COR	10.3	9.85	7.48
Total-PAHs	343	269	229
LMW-PAHs	3.96	2.03	2.13
MMW-PAHs	281	161	122
HMW-PAHs	158	106	105
BbF + BaP + DBA	18.0	10.2	13.6

443, 269, and 229 $\mu g/m^2/day$ at TIP, NCHU, and THU sites, respectively. That is, the dry deposition flux of total PAHs at the industrial site was 1.6 and 1.9 times higher than at the urban and suburban sites. Compared to the results of Sheu *et al.* (1996), the dry deposition fluxes of total PAHs at the industrial and urban sites in central Taiwan are approximately twice those in southern Taiwan. Even the dry deposition flux of total PAHs in the suburban sample area in central Taiwan is almost identical to that of the industrial site of southern Taiwan. High dry deposition flux of total PAHs in

Table 5. Fraction of dry deposition flux from the gas-phase and particle-phase PAHs at the three sampling sites

Compound	TIP		NCHU		THU	
	Gas Phase (%)	Particle Phase (%)	Gas Phase (%)	Particle Phase (%)	Gas Phase (%)	Particle Phase (%)
Nap	91.3	8.70	87.4	12.6	89.2	10.8
AcPy	73.5	26.5	54.2	45.8	67.3	32.7
Acp	28.3	71.7	20.8	79.2	29.0	71.0
Flu	6.00	94.0	5.60	94.4	5.70	94.3
PA	11.8	88.2	14.0	86.0	10.2	89.8
Ant	10.3	89.7	11.1	88.9	14.4	85.6
FL	7.90	92.1	4.80	95.2	6.00	94.0
Pyr	16.7	83.3	30.8	69.2	16.7	83.3
CYC	7.20	92.8	9.20	90.8	11.6	88.4
BaA	14.4	85.6	9.10	90.9	26.8	73.2
CHR	8.00	92.0	6.50	93.5	12.4	87.6
BbF	1.00	99.0	1.00	99.0	0.10	99.9
BkF	1.60	98.4	1.60	98.4	2.20	97.8
PER	0.50	99.5	0.50	99.5	0.80	99.2
BeP	1.10	98.9	0.90	99.1	0.60	99.4
BaP	3.90	96.1	1.70	98.3	3.90	96.1
IND	0.20	99.8	0.20	99.8	0.80	99.2
DBA	0.10	99.9	0.20	99.8	0.30	99.7
BbC	0.20	99.8	0.10	99.9	0.20	99.8
BghiP	0.10	99.9	0.20	99.8	0.80	99.2
COR	0.10	99.9	0.10	99.9	0.10	99.9
Total-PAHs	4.40	95.6	3.69	96.3	4.70	95.3
LMW-PAHs	91.3	8.70	87.4	12.6	90.0	10.0
MMW-PAHs	12.9	87.1	11.5	88.5	13.5	86.5
HMW-PAHs	0.60	99.4	0.50	99.5	0.80	99.2
BbF + BaP + DBA	0.40	99.6	0.50	99.5	0.50	99.5

central Taiwan may be influenced by pollutant sources, distance of pollutant sources from the sampling site and local meteorological conditions. Wind blowing from urban and industrial areas also may carry high concentrations of pollutants, causing the high dry deposition flux of total PAHs in the suburban site. LMW, MMW, and HMW PAHs comprise 0.8%, 63.4%, and 35.8% of the total dry deposition flux at TIP site. The main contribution to total dry deposition flux came from the three to four-ring PAHs, and the contribution of two-ring PAHs comparatively was insignificant. The other two sampling sites displayed the same trend. However, the contribution of HMW PAHs to the dry deposition fluxes of total PAHs exceeded 45% at the THU. Notably, the dry deposition fluxes of BbF + BaP + DBA PAHs were 18, 10.2 and 13.6 $\mu g/m^2/day$ at the TIP, NCHU, and THU, respectively.

According to Sheu *et al.* (1997), the dry

Table 6. Dry deposition velocities for PAH homologue at the three sampling sites

PAH homologue	TIP (cm/sec)	NCHU (cm/sec)	THU (cm/sec)	Mean (cm/sec)
2-ring	0.011	0.008	0.011	0.010
3-ring	0.26	0.23	0.23	0.24
4-ring	0.53	0.36	0.52	0.47
5-ring	0.83	0.62	0.83	0.76
6-ring	0.78	0.94	0.81	0.84
7-ring	0.84	0.95	0.84	0.88
LMW-PAHs	0.011	0.008	0.011	0.01
MMW-PAHs	0.32	0.26	0.30	0.29
HMW-PAHs	0.83	0.66	0.83	0.77
BbF+BaP+DBA	0.80	0.64	1.02	0.82
Total-PAHs	0.24	0.26	0.32	0.27

deposition velocity of gaseous PAHs is in the range of 0.001~0.01 cm/sec. $V_{d,g}$ thus was set as 0.001 cm/sec in this study. Consequently, the dry deposition fluxes of gas-phase and particle-phase PAHs could be calculated using the above equation. Table 5 listed the fraction of dry deposition fluxes contributed by gas-phase and particle-phase PAHs. The dry deposition of total PAHs was contributed mainly by particle-phase, with the contribution from particle-phase ranging between 95.3% and 96.3% at all sampling sites. For LMW PAHs, the gas-phase PAHs contributes 91.3% of the dry deposition flux. Meanwhile, the particle-phase PAHs contributes 88.5% and 86.5% of the dry deposition flux for MMW and HMW PAHs. These higher molecular weight PAHs are deposited primarily by gravitational settling (Sheu *et al.* 1996). The contribution of BbF + BaP + DBA PAHs to dry deposition flux came almost entirely from the particle-phase PAHs, with values of 99.6%, 99.5% and 99.5% at the TIP, NCHU, and THU, respectively.

3.4 Dry Deposition Velocity

The dry deposition velocities of total PAH were 0.24, 0.26 and 0.32 cm/s at the TIP, NCHU and

THU, respectively, and averaged 0.27 cm/s (Table 6). The dry deposition velocity at the THU site was approximately 20% to 30% higher than at the other two sites. This difference could occur because the THU site is located on top of a hill, causing high wind turbulence to and thus a high deposition velocity. The dry deposition velocities of PAH homologue clearly varied from 0.008 to 0.95 cm/s of three sampling sites, and all increased with ring number, except for the six-ring homologue at the TIP. Nevertheless, the mean dry deposition velocities were 0.01, 0.24, 0.47, 0.76, 0.84 and 0.88 cm/s for two to seven-ring PAHs homologue. Notably, the dry deposition velocity of HMW PAHs was considerably higher than that of the LMW PAHs at the three sampling sites. This phenomenon occurs because LMW PAHs mainly distributed in the gas-phase and HMW PAHs primarily associated with the particle-phase (Table 2). Owing to the dry deposition velocities preceded by gravitation settling being much higher than those by diffusion (Holsen *et al.* 1991), HMW PAHs obviously had higher dry deposition velocities than the LMW and MMW PAHs. Moreover, the dry deposition velocities of BbF + BaP + DBA PAHs were 0.8, 0.64 and 1.02 cm/s at the TIP, NCHU, and THU, respectively,

representing an average of 0.82 cm/s. Accordingly, hazardous PAHs with high dry deposition velocities are threatening to human health by dry deposition.

4. Conclusions

Gas-phase and particle-phase PAH concentrations were measured at industrial, urban and suburban sites in central Taiwan. Total PAH concentrations at these sites were 1652, 1185, and 834 ng/m^3, respectively. Combustion activities were the major contributors to PAH concentrations in these areas. PAHs with two to four-ring represented over 94% of total PAHs in the gas-phase of all sampling sites. Meanwhile, PAHs with five to seven-ring represented less than 70% of total PAHs in the gas-phase. Approximately two-thirds of the three most hazardous PAHs (BbF + BaP + DBA) were distributed in the gas-phase of the TIP and NCHU. However, the distribution of BbF + BaP + DBA PAHs was only 36% in the gas-phase at the THU. Total PAH content was 2480, 2230 and 1240 μg/g at the TIP, NCHU and THU, respectively. Notably, total PAH content increased with PAH ring number in all study areas. The dry deposition fluxes of individual PAH ranged from 2.86 to 69.3, 1.90 to 38.6, and 1.55 to 33.1 μg/m^2/day at the TIP, NCHU, and THU, respectively, and the three sites shared very similar profiles. The dry deposition fluxes of total PAHs were 443, 269, and 229 μg/m^2/day at the TIP, NCHU, and THU, respectively. Moreover, 53.3% to 63.4% of the total dry deposition flux was primarily because of the contribution of the three to four-ring PAHs at the three sites. For LMW PAHs, the gas-phase PAHs contributes over 87% to the dry deposition flux at the three sites. On the contrary, the particle-phase PAHs contributes over 86% and 99% of the dry deposition flux of the MMW and HMW PAHs, respectively. The dry deposition velocities of total PAH were 0.24, 0.26 and 0.32 cm/s at the TIP, NCHU and THU, respectively. For two to seven-ring PAH homologue, the mean dry deposition velocities were 0.01, 0.24, 0.47, 0.76, 0.84 and 0.88 cm/s, and increased with PAH ring number. Moreover, HMW PAHs displayed clearly higher dry deposition velocities than those of LMW and MMW PAHs. Finally, the dry deposition velocities of BbF + BaP + DBA PAHs were 0.8, 0.64 and 1.02 cm/s at the TIP, NCHU, and THU, respectively. Accordingly, hazardous PAHs with high dry deposition velocities are threatening to human health by dry deposition.

Acknowledgements

References

Caricchia A. M., Chiavarini S. and Pezza M. (1999), Polycyclic aromatic hydrocarbons in the urban atmospheric particulate matter in the city of Naples (Italy). 33: 3731-3738.

Chetwittayachan T., Shimazaki D. and Yamamoto K. (2002), A comparison of temporal variation of particle-phase polycyclic aromatic hydrocarbons (PAHs) concentration in different urban environments: Tokyo, Japan, and Bangkok, Thailand. Atmos. Environ. 36: 2027-2037.

Fang G. C., Wu Y. S., Chang C. N., Chang K. F. and Yang D. G. (1999), Modeling dry deposition of total particle mass in trafficked and rural sites of central Taiwan. Environ. Int. 25: 625-633.

Georgiadis P. and Kyrtopoulos S. A. (1999), Molecular epidemiological approaches to the study of the genotoxic effects of urban air pollution. Mutat. Res. 428: 91-98.

Holsen T. M., Noll K. E., Liu S. P. and Lee W. J.

(1991), Dry deposition of polychlorinated biphenyls in urban areas. Environ. Sci. Technol. 25: 1075-1081.

Kulkarni P. and Venkataraman C. (2000), Atmospheric polycyclic aromatic hydrocarbons in Mumbai, India. Atmos. Environ. 34: 2785-2790.

Lee W. J., Lewis L. S. J., Chen Y. Y., Wang Y. F., Sheu H. L., Su C. C. and Fan Y. C. (1996), Polychlorinated biphenyls in the ambient air of petroleum refinery, urban and rural areas. Atmos. Environ. 30: 2371-2378.

Li C. S. and Ro Y. S. (2000), Indoor characteristics of polycyclic aromatic hydrocarbons in the urban atmosphere of Taipei. Atmos. Environ. 34: 611-620.

Manoli E., Voutsa D. and Samara C. (2002). Chemical characterization and source identification/apportionment of fine and coarse air particles in Thessaloniki, Greece. Atmos. Environ. 36: 949-961.

Nisbet C. and LaGoy P. (1992), Toxic equivalency factors (TEFs) for polycyclic aromatic hydrocarbons (PAHs). Regul. Toxicol. Pharmacol. 16: 290-300.

Noll K. E. and Fang K. Y. P. (1989), Development of a dry deposition model for atmospheric coarse particles. Atmos. Environ. 23: 585-594.

Park S. S., Kim Y. J. and Kang C. H. (2002), Atmospheric polycyclic aromatic hydrocarbons in Seoul, Korea. Atmos. Environ. 36: 2917-2924.

Sehmel G. A. (1980), Particle and gas dry deposition: A review. Atmos. Environ. 14: 983-1011.

Sheu H. L., Lee W. J., Su C. C., Chao H. R. and Fan Y. C. (1996), Dry deposition of polycyclic aromatic hydrocarbons in ambient air. J. Environ. Eng. 122: 1101-1109.

Sheu H. L., Lee W. J., Lin S. J., Fang G. C., Chang H. C. and You W. C. (1997), Particle-phase PAH content in ambient air. Environ. Pollut. 96: 369-382.

Tsai P. J., Shieh H. Y., Lee W. J. and Lai S. O. (2001), Characteristics of exposure profiles for workers exposed to airborne dusts and polycyclic aromatic hydrocarbons (PAHs) in the carbon black manufacturing industry. J. Occup. Health Psychol. 43: 118-128.

U.S. EPA. (1999), Compendium of Methods for the Determination of Toxic Organic Compounds in Ambient Air. Environmental Protection Agency, US Federal Register, Compendium Method TO-13A, pp.1-42.

WHO, Polynuclear aromatic hydrocarbons (PAHs). (1987), In Air quality guidelines for Europe. Copenhagen, World Health Organization Regional Office for Europe, pp.105-117.